

# Isentropic zonal average formalism and the near-surface circulation

By T.-Y. KOH\* and R. A. PLUMB  
*Massachusetts Institute of Technology, USA*

( 17 May 2004 )

## SUMMARY

The isentropic zonal average formalism is extended to include a rigorous treatment of the bottom boundary of the atmosphere. We define a “surface zone”, where isentropes in the latitudinal plane are interrupted by the Earth’s surface. The zonal average equations of motion and their time average in isentropic coordinates are re-derived in the presence of the surface zone. Applying the extended formalism to a baroclinic wave model, we show that near-surface equatorward mean flow is driven by eastward surface form drag in isentropic coordinates, which in turn is related to poleward geostrophic potential temperature flux at the surface. A potential vorticity - potential temperature picture of extratropical general circulation dynamics above and within the surface zone is presented. We highlight the importance of poleward mean flow in the upper region of the surface zone and investigate the antisymmetric distribution of mean meridional mass flow about the median potential temperature of surface air.

KEYWORDS: angular momentum form drag general circulation heat flux potential vorticity surface zone

## 1. INTRODUCTION

Understanding the general circulation of the Earth’s atmosphere is a major concern in Meteorology. The classical concept of tropospheric general circulation is that it comprises tropical Hadley cells and mid-latitude Ferrel cells. This picture is obtained by performing an Eulerian zonal average in height or pressure coordinates (Holton 1992). The Hadley cell is a direct circulation driven by diabatic heating and constrained by angular momentum conservation (Held and Hou 1980). The Ferrel cell is an indirect circulation driven by eddy transports of momentum and heat. However, the classical concept is not the only way to understand the general circulation. Andrews and McIntyre (1976) formulated the Transformed Eulerian Mean (TEM) formalism, where eddy contributions are removed from the mean circulation by a suitable transformation. Dunkerton (1978) showed that a direct “residual circulation” in the mid-latitudes is obtained in place of the Ferrel cell when the TEM formalism is applied.

Under quasi-geostrophic (QG) assumptions, the TEM formalism sheds much light on the problem of general circulation. For example, the residual circulation is driven by eddy transport of QG pseudo-potential vorticity (e.g. Andrews *et al.* 1987). But for primitive-equation (PE) atmospheres (i.e. assuming only hydrostatic balance in the vertical), it is more insightful from a dynamical point of view to use potential temperature  $\theta$  as the vertical coordinate because under adiabatic inviscid conditions, air flows along isentropic surfaces while conserving Ertel potential vorticity (PV). In isentropic zonal average formalism, the mid-latitude circulation is also direct and is driven by eddy transport of PV (Tung 1986). The analogy between general circulation in  $\theta$ -coordinate PE atmospheres and that in QG atmospheres is evident and useful.

Isentropic analysis of atmospheric circulation has been carried out for many decades now (e.g. Namias 1940). We shall not attempt to summarize all the relevant background literature here, but refer the reader to Section 6.2.1 of Johnson (1989) for a review. We merely note that the general circulation in  $\theta$ -coordinates has been studied before by various investigators (e.g. Dutton 1976, Gallimore and Johnson 1981, Townsend and Johnson 1985, Johnson 1989) in relation to mass, energy, entropy and momentum transport, using both numerical models and data analyses.

\* Present contact: tiehyong@alum.mit.edu

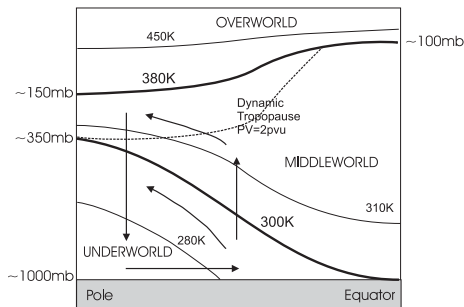


Figure 1. The Overworld, Middleworld and Underworld from Hoskins (1991). Isentropes are shown as thick and thin solid lines, while the dynamic tropopause (i.e.  $PV=2pvu$  contour) is indicated by a dashed line. Arrows represent the isentropic zonal average circulation in the extratropical troposphere after removing the Hadley cell.

The extratropical circulation must be distinguished from the tropical circulation despite both being thermally direct in the isentropic zonal average formalism: the former is primarily forced by baroclinic eddies that prevent the extratropical troposphere from attaining radiative-convective equilibrium; the latter is mainly forced by latent heat release in the Inter-Tropical Convergence Zone (ITCZ) near the equator and net radiative cooling in the subtropical troposphere. Such fundamentally different dynamics is reflected in data analyses showing that the extratropical circulation is largely geostrophic while the tropical circulation is largely ageostrophic (cf. Fig. 8 and 9 of Johnson 1989).

Shaw (1930) was perhaps the first to propose separating the atmosphere into regions (one in each hemisphere) where isentropes intersect the Earth's surface and the region above where isentropes form closed spheroidal surfaces. With the revival of interest in PV dynamics in the last two decades, Hoskins (1991) proposed that a  $PV-\theta$  view be adopted in understanding the general circulation. He divided the atmosphere into three regions (unlike Shaw): (1) the Overworld in the stratosphere (where  $\theta \gtrsim 380$  K); (2) the Middleworld straddling the tropopause (where  $300 \text{ K} \lesssim \theta \lesssim 380 \text{ K}$ ); and (3) the Underworld in the extratropical troposphere (where  $\theta \lesssim 300$  K). (See Fig. 1.) The tropical troposphere is excluded from the Underworld because of weak horizontal temperature gradients. This paper is concerned with the extratropical circulation, particularly that near the surface. Therefore, our focus is on the Underworld.

Held and Schneider (1999) argued that the equatorward branch of the circulation near the surface provides an important link to understanding extratropical general circulation. The argument was made as follows: the equator-pole temperature gradient at the surface determines the eddy heat flux near the surface through an eddy-diffusion mechanism (Held 1999). Then, the poleward eddy heat flux forces an equatorward mean flow near the surface in the temperate zone. The horizontal convergence of the near-surface mean flow acts like a mass source in subtropical latitudes for quasi-isentropic ascent within the extratropical troposphere. Eventually, radiative cooling causes air to descend back towards the surface. In an equilibrated climate, the equatorward mean flow near the surface must balance the PV-flux-driven poleward mean flow in the extratropical atmosphere. (That poleward mean flow is strongest at the tropopause level where mean PV gradients along isentropes are concentrated.) In other words, there is a balance between poleward surface heat flux and equatorward eddy PV flux in the atmosphere.

The above view of the extratropical general circulation demands a proper understanding of near-surface dynamics. In Section 2, it is noted that the existing isentropic

zonal average formalism introduces fictitious forces into the horizontal momentum equations at the surface. This is not satisfactory for our purpose of relating the mean meridional flow to surface heat flux and interior PV flux. Hence, we extend the existing formalism to include the surface boundary in a way that respects the surface dynamics without inventing “underground” meteorological quantities. We test the extended formalism by applying it to a baroclinic wave model described in Section 3. We examine angular momentum balance and surface heat transport in the mid-latitudes of this model atmosphere in Section 4. The objective is to elucidate synoptic-scale and longer-time dynamics that drive the near-surface circulation in  $\theta$ -coordinates. Then, motivated by a kinematic argument put forth in Held and Schneider (1999), we use the time-average formalism to investigate the climatological structure of the near-surface circulation. The main findings of this paper are summarized in our conclusions in Section 5.

## 2. ISENTROPIC ZONAL AVERAGE FORMALISM

Zonal average equations in  $\theta$ -coordinates can be found in e.g. Andrews *et al.* (1987). The derivation of these equations often assumes that isentropes are closed surfaces, which is true in the Overworld and Middleworld. However, in the Underworld, isentropic surfaces are interrupted by the Earth’s surface. A few authors (e.g. Andrews 1983, Johnson 1989, Held and Schneider 1999) have devised ways to deal with this, based on the convention in Lorenz (1955) where isentropes upon meeting the surface are assumed to continue just below the surface. Thus, pressure and horizontal velocities are set to surface values and mass density is put to zero on the “underground” isentropes.

Andrews (1983) noted that while following the Lorenz convention, the horizontal momentum equations are not satisfied on “underground” isentropes, or equivalently, fictitious underground body forces are introduced. The same may be said of the approach in Johnson (1989) where non-slip surface boundary conditions were assumed, or in Held and Schneider (1999) where only underground geostrophic winds were considered. However, as these authors were considering mass-weighted averages and mass density is zero underground, underground momentum contributions and the fictitious forces are absent in the zonal average equations.

All approaches to deal with isentropes intersecting the surface are mathematical constructs. Their usefulness depends on to what use they are put. In this paper, we want to relate angular momentum transport to PV fluxes. It will become clear in subsection (c) that a non-weighted zonal mean angular momentum equation suits our purpose. Therefore, we must devise an alternative treatment of isentropes intersecting the surface that does not introduce fictitious forces into the horizontal momentum equations.

### (a) Basic Definitions

In  $\theta$ -coordinates, the bottom surface of the atmosphere  $\theta = \theta_a(\lambda, \varphi, t)$  undulates in the horizontal, and the undulations vary with time. In a vertical-zonal plane, isentropes are sometimes “below” the Earth’s surface (see Fig. 2). One way to avoid the mentioned fictitious “underground” forces in the momentum equations is to abandon the Lorenz convention and treat only isentropic layers that exist physically in the atmosphere.

Let us denote the minimum and maximum potential temperature of air at the Earth’s surface at latitude  $\varphi$  and time  $t$  by  $\theta_{\min}(\varphi, t)$  and  $\theta_{\max}(\varphi, t)$  respectively. So, one may define a “surface zone” where  $\theta_{\min} \leq \theta \leq \theta_{\max}$ . The top of the surface zone  $\theta_{\max}$  may vary greatly in geopotential height, but such variation is implicit in isentropic averaging. Within the surface zone, isentropic layers are disjointed tubes in the zonal direction, i.e. the segments where  $\theta < \theta_a$  do not exist at all.

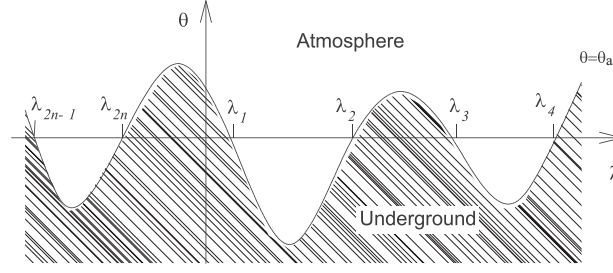


Figure 2. The undulating bottom surface of the atmosphere shown in the  $(\lambda, \theta)$ -plane. Intersections between the isentrope  $\theta$  and the Earth's surface are labelled  $\{\lambda_j : j = 1, 2, \dots, 2n\}$ .

Held and Schneider (1999) defined practically the same notion of the surface zone but called it the “surface layer”. We avoid their terminology, lest it be confused with the same terminology used in boundary-layer meteorology that refers to the atmospheric layer next to the surface where turbulent momentum fluxes are constant (e.g. Holton 1992). The surface zone and the turbulent boundary layer are independent concepts.

Let us define a normalized zonal sum  $\bar{A}^S$  for some quantity  $A(\lambda, \varphi, \theta, t)$  as

$$\bar{A}^S \equiv \frac{1}{2\pi} \sum_{i=1}^n \int_{\lambda_{2i-1}}^{\lambda_{2i}} A d\lambda = \frac{1}{2\pi} \int_0^{2\pi} A \mathcal{H}\{\theta - \theta_a(\lambda)\} d\lambda \quad (1)$$

where  $\{\lambda_j : j = 1, 2, \dots, 2n\}$  are defined in Fig. 2, and  $\mathcal{H}$  is the Heaviside step function, defined here as 0 for  $x \leq 0$  and 1 for  $x > 0$ . The above definition excludes all points where  $\theta < \theta_a$ . So the fraction of latitude circle on an isentropic surface in the atmosphere is

$$\varpi \equiv \bar{1}^S$$

Above the surface zone,  $\varpi = 1$ , while within the surface zone,  $0 < \varpi < 1$ . Note the following definitions for zonal averages and deviations for regions where  $\varpi \neq 0$ :

$$\bar{A} \equiv \bar{A}^S / \bar{1}^S \quad (2)$$

$$\bar{A}^* \equiv (\overline{\sigma A})^S / \bar{\sigma}^S \quad (3)$$

$$A' \equiv A - \bar{A} \quad (4)$$

$$A^\dagger \equiv A - \bar{A}^* \quad (5)$$

where  $\sigma \equiv -g^{-1} \partial p / \partial \theta$  is the mass density in  $\theta$ -coordinates. With these definitions, the familiar identities are still valid:  $\overline{AB} \equiv \bar{A}\bar{B} + \overline{A'B'}$  and  $\overline{AB}^* \equiv \bar{A}^*\bar{B}^* + \overline{A^\dagger B^\dagger}^*$ .

(Notation: overbars with or without superscripts always indicate zonal averages, primes and daggers denote deviations from non-weighted and mass-weighted averages respectively, while tildes  $\sim$  distinguish specially defined zonal averages.)

In using  $\theta$ -coordinates, the presence of neutrally stable or mixed layers poses a minor complication. A mixed layer is represented by a 2D surface in  $\theta$ -coordinates and the isentropic density  $\sigma$  on that surface is infinite. In this case, the above definition for  $\bar{A}^S$  is still valid, provided a local coordinate transform is performed for the contribution

to the integral at the longitude  $\lambda_{mix}$  where the isentrope encounters the mixed layer:

$$\int_{\substack{\lambda_{mix}-\epsilon \\ \theta=\text{const.}}}^{\lambda_{mix}+\epsilon} A d\lambda = \int_{\substack{p_- \\ \theta=\text{const.}}}^{p_+} A \left( \frac{\partial p}{\partial \lambda} \right)_\theta^{-1} dp = \frac{1}{g} \int_{\substack{p_- \\ \lambda=\lambda_{mix}}}^{p_+} \frac{A}{\sigma} \left( \frac{\partial \theta}{\partial \lambda} \right)_p^{-1} dp \quad (6)$$

where  $\epsilon$  is an arbitrarily small positive number and the mixed layer extends from  $p_-$  to  $p_+$  in  $p$ -coordinates ( $(\partial\theta/\partial\lambda)_p > 0 \Leftrightarrow p_+ > p_-$ ). Note that  $A/\sigma$  can be either zero (e.g.  $A = u$ ) or finite (e.g.  $A = \sigma v$ ) in the mixed layer. Thus, for instance, mixed layer contributions are excluded from  $\bar{u}$ , but included in  $\bar{v}^*$ .

### (b) Surface Zone Equation

As the atmosphere's bottom surface is not rigid in  $\theta$ -coordinates, the surface zone moves around in  $(\varphi, \theta)$ -space with time, or in other words  $\varpi$  varies with time.

Suppose in a vertical-zonal plane, an isentropic tube of air in the surface zone meets the surface at  $2n$  points with longitudes  $\lambda_j(\varphi, \theta, t)$ . Without loss of generality, we may assume that the atmosphere exists east of odd- $j$  points and west of even- $j$  points (Fig. 2). From the definition of diabatic heating of surface air and elementary manipulations of the partial derivatives of surface air potential temperature, one may prove that

$$\frac{u_a(\lambda_j)}{a \cos \varphi} \equiv \frac{\partial \lambda_j}{\partial t} + \frac{v_a(\lambda_j)}{a} \frac{\partial \lambda_j}{\partial \varphi} + Q_a(\lambda_j) \frac{\partial \lambda_j}{\partial \theta} \quad (7)$$

where  $a$  is Earth's radius,  $(u_a, v_a)$  is the horizontal wind at the surface and  $Q_a$  is the surface diabatic heating rate expressed as the rate of increase in potential temperature following a surface air parcel. The subscripts  $a$  denote values at the bottom of the atmosphere. For notational simplicity, we shall henceforth write  $A_j$  to mean  $A_a(\lambda_j)$ . Thus,

$$\frac{\partial \varpi}{\partial t} = \frac{-1}{2\pi} \sum_{i=1}^n \left[ Q_j \frac{\partial \lambda_j}{\partial \theta} + \frac{v_j}{a} \frac{\partial \lambda_j}{\partial \varphi} - \frac{u_j}{a \cos \varphi} \right]_{j=2i-1}^{j=2i} \quad (8)$$

We may loosely call the above equation the ‘‘surface zone equation’’. It is effectively a lower boundary condition for the zonal average atmosphere in  $\theta$ -coordinates.

If one randomly selects a point on the Earth's surface at latitude  $\varphi$  and time  $t$ , the probability of finding an air parcel with potential temperature between  $\theta$  and  $\theta + \delta\theta$  is  $\mu(\theta) \delta\theta \equiv (2\pi)^{-1} \sum_{j=1}^{2n} |\delta\lambda_j| = \delta\varpi$ , where  $\delta\lambda_j$  is the change in  $\lambda_j$  corresponding to the change  $\delta\theta$ . (Note that from Fig. 2, for positive  $\delta\theta$ ,  $\delta\lambda_j$  is negative for odd  $j$  and positive for even  $j$  as static stability is non-negative.) Hence, the probability density is

$$\mu(\theta) \equiv \frac{1}{2\pi} \sum_{j=1}^{2n} (1/r)_{\lambda=\lambda_j} = \frac{\partial \varpi}{\partial \theta} \quad ; \quad r \equiv \left| \frac{\partial \theta_a}{\partial \lambda} \right| \quad (9)$$

Thus,  $\varpi(\theta)$  is the probability distribution of surface air potential temperature: it is the probability that a surface air parcel is potentially cooler than  $\theta$  at latitude  $\varphi$  and time  $t$ . The expectation for a property  $A(\lambda, \varphi, t)$  associated with a surface air parcel that has potential temperature  $\theta$  at latitude  $\varphi$  and time  $t$  is

$$E(A) \equiv \frac{\sum_{j=1}^{2n} (A/r)_{\lambda=\lambda_j}}{\sum_{j=1}^{2n} (1/r)_{\lambda=\lambda_j}} \quad (10)$$

Using Eq. (9) and (10), Eq. (8) becomes

$$\frac{\partial \varpi}{\partial t} = -\mu(\theta) \left\{ E(Q_a) + E \left( -\frac{v_a}{a} \frac{\partial \theta_a}{\partial \varphi} - \frac{u_a}{a \cos \varphi} \frac{\partial \theta_a}{\partial \lambda} \right) \right\}$$

So the cooling of surface air at potential temperature  $\theta$  (due to either diabatic processes or advection) determines how much more surface air will be potentially cooler than  $\theta$ , and hence the increase in the probability  $\varpi$  of finding a surface air parcel with potential temperature less than  $\theta$ . This is the physical basis for the surface zone equation (8).

For later reference, let us define an operator  $\tilde{D}$  and rewrite equation (8) as

$$\begin{aligned} \tilde{D} &\equiv \partial/\partial t + a^{-1} \bar{v}^* \partial/\partial \varphi + \bar{Q}^* \partial/\partial \theta \\ \tilde{D} \varpi &= \frac{-1}{2\pi} \sum_{i=1}^n \left[ Q_j^\dagger \frac{\partial \lambda_j}{\partial \theta} + \frac{v_j^\dagger}{a} \frac{\partial \lambda_j}{\partial \varphi} - \frac{u_j'}{a \cos \varphi} \right]_{j=2i-1}^{j=2i} \end{aligned} \quad (11)$$

(c) *Angular Momentum Equation*

Schär (1993) writes the zonal momentum equation in  $\theta$ -coordinates as

$$\frac{\partial u}{\partial t} - \zeta_\theta v + Q \frac{\partial u}{\partial \theta} - F_\lambda = \frac{-1}{a \cos \varphi} \frac{\partial B}{\partial \lambda} \quad (12)$$

where  $\zeta_\theta$  is the absolute vorticity normal to an isentropic surface and  $F_\lambda$  is the zonal turbulent drag.  $B \equiv M + (u^2 + v^2)/2$  is the Bernoulli function in  $\theta$ -coordinates.  $M \equiv \theta \Pi(p) + \Phi$  is Montgomery potential, where  $\Phi$  is geopotential and  $\Pi(p) \equiv c_p(p/1000 \text{ mb})^\kappa$  is Exner's function ( $\kappa \equiv R/c_p$ ). Haynes and McIntyre (1987, 1990) put forth the concept of a "potential vorticity substance" whose mixing ratio is PV, and whose transport is always along isentropes. The flux of PV substance comprises an advective component  $\zeta_\theta \mathbf{v}$  and a non-advective component  $\mathbf{k} \times (\mathbf{F} - Q \partial \mathbf{v} / \partial \theta)$  due to drag  $\mathbf{F}$  and diabatic heating  $Q$ . Thus, Schär's equation is a statement that zonal acceleration is caused by meridional transport of PV substance and a Bernoulli force.

Let us introduce  $L \equiv \Omega a \cos^2 \varphi + u \cos \varphi$ , where  $La$  is the absolute angular momentum per unit mass about the Earth's rotation axis. Taking the normalized zonal sum of  $\cos \varphi \times$  Eq. (12), one obtains after some algebraic manipulations,

$$\frac{\partial \bar{L}^S}{\partial t} + \frac{\bar{v}^*}{a} \frac{\partial \bar{L}^S}{\partial \varphi} + \bar{Q}^* \frac{\partial \bar{L}^S}{\partial \theta} = \left( \overline{\sigma v^\dagger \xi^\dagger}^S - \overline{Q^\dagger \frac{\partial u}{\partial \theta}}^S + \overline{F_\lambda}^S \right) \cos \varphi + G \quad (13)$$

where  $\xi \equiv \zeta_\theta / \sigma$  is PV and  $G$  represents surface boundary terms. Mixed-layer contributions are found in  $\bar{v}^*$ ,  $\bar{Q}^*$ ,  $\overline{\sigma v^\dagger \xi^\dagger}^S$  and  $\overline{Q^\dagger \partial u / \partial \theta}^S$ . From  $\bar{L}^S = \varpi \bar{L}$  and Eq. (11),

$$\left( \frac{\partial}{\partial t} + \frac{\bar{v}^*}{a} \frac{\partial}{\partial \varphi} + \bar{Q}^* \frac{\partial}{\partial \theta} \right) \bar{L} a = J + G_A + G_B \quad (14)$$

$$J \equiv \left( \overline{\sigma v^\dagger \xi^\dagger} - \overline{Q^\dagger \frac{\partial u}{\partial \theta}} + \overline{F_\lambda} \right) a \cos \varphi \quad (15)$$

$$G_A \equiv \frac{1}{2\pi \varpi} \sum_{i=1}^n \left[ \left( \frac{u_j'}{a \cos \varphi} - \frac{v_j^\dagger}{a} \frac{\partial \lambda_j}{\partial \varphi} - Q_j^\dagger \frac{\partial \lambda_j}{\partial \theta} \right) u_j' a \cos \varphi \right]_{j=2i-1}^{j=2i} \quad (16)$$

$$G_B \equiv \frac{-1}{2\pi \varpi} \sum_{i=1}^n \left[ M_j' + \frac{u_j'^2 + v_j^{\dagger 2}}{2} \right]_{j=2i-1}^{j=2i} \quad (17)$$

$J$  is the PV flux along isentropes due to eddy transport, eddy diabatic heating and mean turbulent drag.  $G_A$  is the eddy advection of eddy angular momentum at the surface (Appendix A).  $G_B$  is an eddy Bernoulli term, dominated by the mean pressure torque  $G_M$  or equivalently the analogous surface form drag in  $\theta$ -coordinates (Appendix B):

$$G_M \equiv \frac{-1}{2\pi\varpi} \sum_{i=1}^n [M'_j]_{j=2i-1}^{j=2i} = -\frac{\overline{\partial M}}{\partial \lambda} \quad (18)$$

As  $\varpi$  approaches zero, i.e. as the zonal extent of an isentropic tube in the atmosphere shrinks to zero,  $G_A$ ,  $G_B$  and  $G_M$  remain finite because  $M$ ,  $u$ ,  $v$  and  $Q$  are smooth functions and tend to their mean values and so their deviations tend to zero.

**The three effects represented by  $J$ ,  $G_B$  and  $G_A$  alter the mean absolute angular momentum and force a circulation normal to the contours of  $\bar{L}$ .**  $J$  is well-known in the literature, although it may be written in various forms, e.g. Eq. (4.6) of Tung (1986) and Eq. (3.9.9) of Andrews *et al.* (1987).  $G_A$  and  $G_B$  are of course non-zero only in the surface zone, and we are not aware of previous literature that explicitly identifies them. The simple form and physical interpretation of  $G_A$  and  $G_B$  are consequences of using our definition of zonal averages in the surface zone.

#### (d) Other Equations

For completeness, we briefly present the other zonal average equations describing the general circulation in  $\theta$ -coordinates that were derived in Koh (2001):

$$\frac{\partial}{\partial t} \bar{\sigma}^S + \frac{1}{a \cos \varphi} \frac{\partial}{\partial \varphi} \bar{\sigma}^S \bar{v}^* \cos \varphi + \frac{\partial}{\partial \theta} \bar{\sigma}^S \bar{Q}^* = 0 \quad (19)$$

$$\frac{\partial}{\partial \theta} \left( f + \frac{\bar{u}}{a} \tan \varphi \right) \bar{u} + \frac{1}{a} \frac{\partial}{\partial \varphi} \left( \kappa + \frac{1 - \kappa}{\varpi} \right) \Pi(\bar{p}) = \frac{\partial}{\partial \theta} \left( \bar{F}_\varphi^* - \bar{D}\bar{v}^* \right) + \Delta \quad (20)$$

Equation (19) demonstrates mass continuity, where  $\bar{\sigma}^S$  is proportional to the mass of air in the isentropic tube  $\delta\theta$  at latitude  $\varphi$ . The derivation is straightforward: take the normalized zonal sum of the continuity equation in  $\theta$ -coordinates and use Eq. (7).

In Eq. (20), terms involved in gradient wind balance are grouped together on the LHS. The nonlinearity of Exner's function makes a difference to the pressure term in the surface zone.  $\Delta$  on the RHS denotes a plethora of surface boundary terms, second- and third-order eddy covariances (between  $u'$ ,  $v^\dagger$ ,  $Q^\dagger$ ,  $\sigma'$  and  $\partial M'/\partial \varphi$ ) representing meridional momentum transport, and second- and higher-order eddy covariances of  $p'$  that arise from the nonlinearity of Exner's function. Apart from the lower region of the surface zone where meridional turbulent drag  $\bar{F}_\varphi^*$  and surface boundary effects are strong, gradient wind balance is generally a good approximation (i.e. RHS  $\approx 0$ ).

#### (e) Time-Average Formulation

Suppose one takes the time average of zonally averaged data to study the atmosphere's climatology. Starr and White (1951) showed that transient axisymmetric contributions are not important to the atmosphere's angular momentum budget in pressure coordinates. In fact, one can understand the climatological general circulation as though it were a steady-state solution of the zonal average equations (e.g. Andrews *et al.* 1987, Holton 1992). But as we are examining the general circulation in  $\theta$ -coordinates, where the surface boundary is replaced by a surface zone, care was taken to derive a time-average formulation for the isentropic zonal average equations.

To keep this paper concise, we refer the interested reader to Koh (2001) for the time-average isentropic zonal average equations, providing only an outline here. The climatological surface zone spans the range of potential temperature fluctuations of surface air for all longitudes at latitude  $\varphi$  over the time interval  $[t_\alpha, t_\beta]$  under consideration. We define the normalized temporal sum as:

$$\langle A \rangle^S (\lambda, \varphi, \theta) \equiv \frac{1}{t_\beta - t_\alpha} \sum_{j=1}^m \int_{t_{2j-1}}^{t_{2j}} A (\lambda, \varphi, \theta, t) dt \quad (21)$$

where  $[t_{2j-1}, t_{2j}] \subseteq [t_\alpha, t_\beta]$  is the  $j$ th time interval for which  $\theta_a (\lambda, \varphi, t) \leq \theta$  (or  $\varpi (\varphi, \theta, t) > 0$  if  $A$  is independent of  $\lambda$ ). The temporal mean  $\langle A \rangle$  and the mass-weighted temporal mean  $\langle A \rangle^*$  can be defined using the normalized temporal sum (with  $A$  suitably weighted with  $\bar{1}^S$  and  $\bar{\sigma}^S$  respectively if  $A$  is independent of  $\lambda$ ). Anomalies  $A'$  and  $A^\dagger$  are now defined respectively with respect to the temporal zonal mean  $\langle \bar{A} \rangle$  and the mass-weighted temporal zonal mean  $\langle \bar{A}^* \rangle^*$  which replace  $\bar{A}$  and  $\bar{A}^*$ . The probability distribution of surface air potential temperature is  $\langle \varpi \rangle^S$ . The definitions for  $E$ ,  $G_A$ ,  $G_B$  and  $G_M$  are like in Eq. (10), (16), (17) and (18) respectively but for additionally taking temporal sums in the numerator and denominator. The time-average zonal average equations for an equilibrated atmosphere was proven to be exactly analogous to the zonal average equations with time tendencies put to zero.

### 3. BAROCLINIC WAVE MODEL

To see how the extended isentropic formalism performs as a diagnostic tool, we employ the stylized model of mid-latitude baroclinic wave dynamics of Thorncroft *et al.* (1993). The circulation in a baroclinic-wave life-cycle can be viewed as the circulation of a cyclone-anticyclone pair within a baroclinic wave packet in the atmosphere (Lee and Held 1993). Thus, the nonlinear baroclinic-wave life-cycle is able to exemplify the basic character of synoptic disturbances in the mid-latitude troposphere.

Breaking with the practice of using adiabatic, frictionless life-cycles (e.g. Simmons and Hoskins 1978), we investigated a model that has simple parameterizations for surface fluxes of heat and momentum, boundary-layer turbulence, dry convection and radiative heating. However, no explicit representation of water vapor and its effects have been incorporated, as a proper account for these effects deserves a separate more in-depth study. For the sake of simplicity, the model also does not contain any topography or land-sea contrast, even though these factors influence the circulation in the mid-latitudes (e.g. Davis 1997, Hoskins and Valdes 1990).

The numerical model is global in extent and employs T63 pseudo-spectral representation of  $\sigma_p$ -coordinate primitive equations (Bourke 1974, Hoskins and Simmons 1975), where  $\sigma_p$  is the ratio of pressure to surface pressure. There are 17 vertical levels, 3 of which lies in the planetary boundary layer (PBL) that extends from the surface to  $\sigma_p = 0.866$ . Appendix C gives further details of the model numerics and physics.

#### (a) Basic State and Initial Perturbation

The baroclinic-wave life-cycle is essentially an initial-value problem where the initial basic state (Fig. 3(a)) of the model atmosphere is baroclinically unstable. The basic state has a PBL that is virtually statically neutral in the extratropics. Above the PBL, it is identical to that used in Thorncroft *et al.*'s baroclinic-wave life-cycle LC1. The tropopause has a realistic slope in the mid-latitudes, but the tropospheric stratification

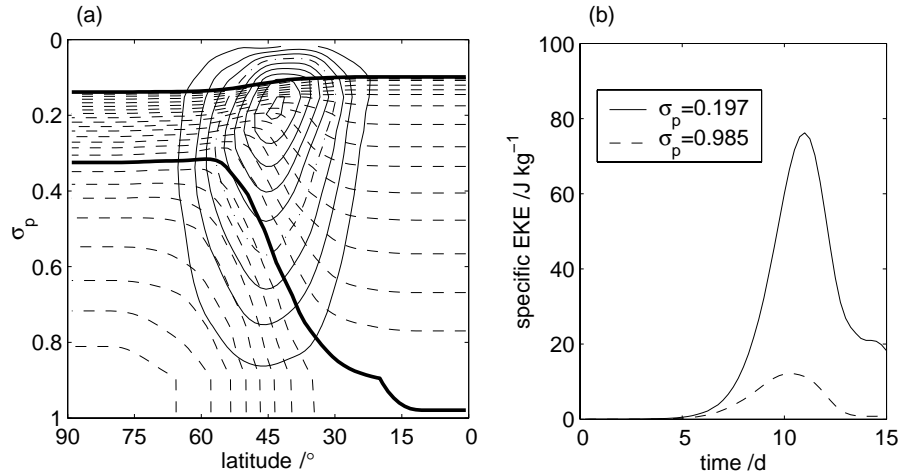


Figure 3. (a) Initial basic state of the baroclinic wave model, showing the distribution of potential temperature (dashed contours at intervals of 5K) and zonal wind (solid contours at intervals of 5m/s). Thick solid lines denote the 300K- and 380K-isentropes. The dash-dot line indicates the 20m/s-contour for zonal wind. (b) Growth of the specific eddy kinetic energy (EKE) in the tropopause region ( $\sigma_p = 0.197$ ) and just above the surface ( $\sigma_p = 0.985$ ) in the baroclinic-wave life-cycle.

increases unrealistically with altitude. The jet position and strength is not inconsistent with what is seen in the Pacific storm track east of Japan during winter. The basic state observes gradient wind balance and hydrostatic balance.

To obtain a baroclinic wave life-cycle akin to Thorncroft *et al.*'s life-cycle LC1, we used an analytic zonal wavenumber-six perturbation in the initial surface pressure  $p_{s0}$ :

$$\ln(p_{s0}/p_{ref}) = 10^{-3}(Y_7^6 + 0.7Y_9^6) \quad (22)$$

where  $p_{ref}$  is the reference global mean surface pressure and  $Y_n^m$  is the spherical harmonic of total wavenumber  $n$  and zonal wavenumber  $m$ , normalized such that its global mean square value is  $2\pi$ .  $p_{s0}$  was chosen so that its initial projection into the most unstable mode is large enough for the most unstable mode to grow and dominate all other modes before the model exits the linear regime. For the next 15 days, the model practically behaves as if it were initialized with the most unstable normal mode.

### (b) Baroclinic-wave Life-cycle

Figure 3(b) shows the baroclinic-wave life-cycle going through stages of exponential growth (Day 0 to Day 9), nonlinear saturation (Day 9 to Day 11) and nonlinear decay (Day 11 to Day 14). The synoptic development of baroclinic waves may be described most simply as the interaction of two wave-trains of PV anomalies: one at the surface and the other at the tropopause level (Hoskins *et al.* 1985). The growth and decay of the wave leads to (incomplete) stabilization of the mean flow with respect to baroclinic instability. Such a description suffices for our purpose. More involved analyses e.g. based on Eliassen-Palm fluxes and ray-tracing techniques can be found in Thorncroft *et al.* (1993), and based on wave activity can be found in Magnusdottir and Haynes (1996).

For presentation purpose, we shall focus on the baroclinic wave at Day 10 (not shown), just before the wave saturates. Cyclones and anticyclones, and warm and cold fronts are well-developed by this time. The breaking of high-PV filaments and intensification of the jet stream at the tropopause are also underway.

(c) *Long-time Integration*

While baroclinic-wave life-cycles are useful paradigms for studying mid-latitude eddies over synoptic scales, as solutions to initial-value problems they do not represent an equilibrated atmospheric state even when averaged over their life spans. Therefore, a 300 day-integration of the baroclinic wave model was carried out to investigate mid-latitude circulation in an equilibrated atmosphere. The initial basic atmospheric profile, numerical and physical parameters used for this experiment are identical to those used for the baroclinic-wave life-cycle. The initial condition in this case takes the form

$$\ln(p_{s0}/p_{ref}) = C_0 - 0.03 \sin^2 2\varphi \exp\{-9(\lambda - \pi)^2 / 4\pi^2\}$$

where the constant  $C_0$  is chosen to keep the hemispheric average of  $\ln(p_{s0}/p_{ref})$  at zero or the global mean surface pressure at  $p_{ref}$ . The zonally Gaussian disturbance evolves into a wave packet that eventually occupies the entire latitude circle.

## 4. RESULTS AND DISCUSSIONS

(a) *Momentum Balance*

Equation (14) may be rewritten showing only dominant terms:

$$\tilde{D}(\bar{u} \cos \varphi) = f\bar{v}^* \cos \varphi + \overline{\sigma v^\dagger \xi^\dagger} \cos \varphi + a^{-1} G_M + \dots \quad (23)$$

The terms are from left to right: relative torque (i.e. rate of change of mean relative angular momentum), Coriolis force, eddy PV flux and surface form drag in  $\theta$ -coordinates.

In the region above the surface zone, surface form drag is absent by definition. Figure 4 shows that mean zonal wind  $\bar{u}$  in this region is decelerated by negative drag due to equatorward eddy PV flux, and accelerated or decelerated by the Coriolis force  $f\bar{v}^* \cos \varphi$  depending on the sign of mean meridional flow  $\bar{v}^*$ . The atmosphere is not in steady state over synoptic time-scales, and so balance between eddy PV flux and Coriolis force cannot be assumed on such time-scales.

Within the surface zone, Fig. 4 shows that relative torque is negligible and eddy PV flux is weak. Thus, one may understand the near-surface equatorward mean flow as dynamically driven by the balance between eastward surface form drag and westward Coriolis force. The fact that surface form drag in  $\theta$ -coordinates is eastward may be explained by Fig. 5. Equatorward advection of potentially cold air depresses the Earth's surface in  $\theta$ -coordinates, creating a "valley" in the surface zone. Geostrophic balance means that the western "valley wall" is at a higher pressure than the eastern "valley wall" at the same  $\theta$ -level. Since  $M \equiv \theta \Pi(p) + \Phi$ , an eastward surface form drag results in the absence of surface topography. The effect of topography will be discussed later.

The preceding explanation is not the only way to understand the isentropic zonal average circulation in the extratropics. Gallimore and Johnson (1981) considered the mass-weighted zonal mean angular momentum  $\bar{L}^*$  (as opposed to the non-weighted zonal mean  $\bar{L}$  above) and showed that

$$\left( \frac{\partial}{\partial t} + \frac{\bar{v}^*}{a} \frac{\partial}{\partial \varphi} + \bar{Q}^* \frac{\partial}{\partial \theta} \right) \bar{L}^* a = \bar{F}_\lambda^* a \cos \varphi - \frac{\overline{\partial M}}{\partial \lambda} - \frac{1}{\bar{\sigma}^S} \nabla^{(\theta)} \cdot \mathbf{E} \quad (24)$$

$$\mathbf{E} \equiv \overline{(\sigma u^\dagger v^\dagger)^S} a \cos^2 \varphi, \overline{(\sigma u^\dagger Q^\dagger)^S} a \cos \varphi \quad (25)$$

where  $\mathbf{E}$  is the eddy angular momentum flux in  $\theta$ -coordinates and the divergence operator  $\nabla^{(\eta)}$  acting on a vector  $\mathbf{U} \equiv (U_\varphi, U_\eta)$  in generalized  $\eta$ -coordinates on a sphere

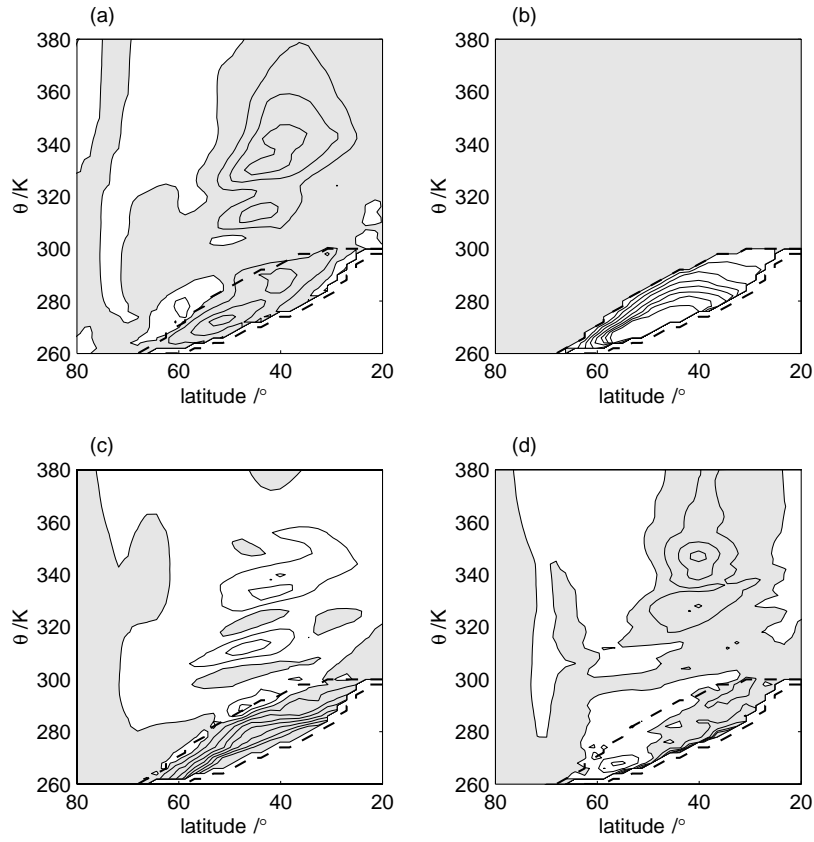


Figure 4. The dominant terms at Day 10: (a) eddy PV flux  $\overline{\sigma v^{\dagger} \xi^{\dagger}} \cos \varphi$ , (b) surface form drag in  $\theta$ -coordinates  $G_M/a$ , (c) Coriolis force  $f\bar{v}^* \cos \varphi$  and (d) relative torque  $\tilde{D}(\bar{u} \cos \varphi)$ . The contour interval is  $0.02\Omega a/\text{day}$  in the range  $-0.1\Omega a/\text{day}$  to  $0.1\Omega a/\text{day}$ . The surface zone is demarcated by dashed lines.

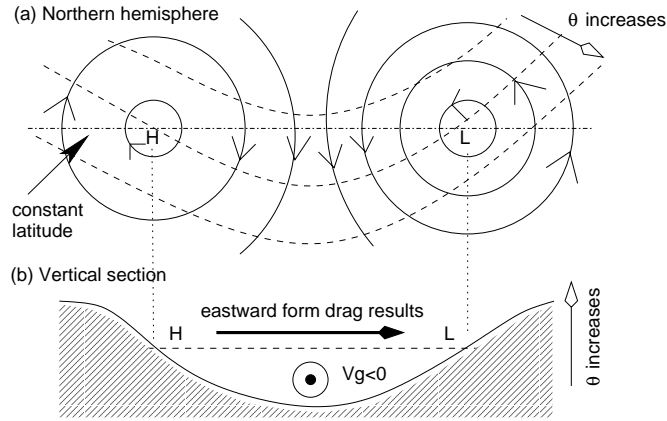


Figure 5. (a) A surface cyclone-anticyclone pair in the northern mid-latitudes, where geostrophic winds are indicated by arrows and surface isentropes are represented by dashed contours; (b) Earth's surface in a vertical cross-section at constant latitude (denoted by the dash-dot line in (a)) in  $\theta$ -coordinates.

is given by  $\nabla^{(\eta)} \cdot \mathbf{U} \equiv (a \cos \varphi)^{-1} \partial U_\varphi / \partial \varphi + \partial U_\eta / \partial \eta$ . Appendix D shows that mass-weighted zonal mean pressure force,  $-(a \cos \varphi)^{-1} \overline{\partial M / \partial \lambda^*}$ , is synonymous to form drag or net pressure stress exerted on an isentropic tube by the surrounding atmosphere ( $F_D$ ) and by the Earth's surface ( $F_S$ ).  $F_S$  can be non-zero only in the surface zone.

The dominant terms in Eq. (24) on synoptic time-scales in the extratropics are relative torque, Coriolis force (planetary angular momentum advection) and form drag:

$$\tilde{D}(\bar{u}^* \cos \varphi) = f \bar{v}^* \cos \varphi + (F_D + F_S) \cos \varphi + \dots \quad (26)$$

In this framework, the acceleration of the mean flow is the result of Coriolis force and form drag. Within the surface zone, the acceleration is negligible and so Coriolis force balances pressure stresses exerted by both the surrounding atmosphere and by the Earth's surface. (In our model, there is no surface topography and so the surface pressure stress has zero horizontal component, i.e.  $F_S = 0$ .)

Comparing Eq. (23) and (26), we deduce that

$$\overline{\sigma v^\dagger \xi^\dagger} + (a \cos \varphi)^{-1} G_M \approx F_D + F_S \quad (27)$$

This type of relation between PV flux and form drag is not new. For isentropic surfaces uninterrupted by the Earth's surface, Tung (1986) showed that

$$\overline{\sigma v^\dagger \xi^\dagger} \approx \frac{1}{\bar{\sigma} \cos \varphi} \left\{ \nabla^{(\theta)} \cdot \mathbf{F}_{EP}^{(\theta)} - \frac{\partial}{\partial t} (\overline{\sigma' u'}) \cos \varphi \right\} \quad (28)$$

$$\mathbf{F}_{EP}^{(\theta)} \equiv \left\{ -(\overline{\sigma v})' u' \cos^2 \varphi, -(\overline{\sigma Q})' u' \cos \varphi + \frac{1}{a} p' \frac{\partial z'}{\partial \lambda} \right\} \quad (29)$$

The divergence of the second term in the vertical component of Eliassen-Palm flux  $\mathbf{F}_{EP}^{(\theta)}$  is the dominant term on the RHS of Eq.(28) and it is the form drag  $F_D$  exerted on the isentropic layer by the surrounding atmosphere. Within the surface zone, Eq. (27) shows that additional form drag from the Earth's surface  $F_S$  and the different but analogous surface form drag in  $\theta$ -coordinates  $(a \cos \varphi)^{-1} G_M$  contribute to the balance as well.

### (b) Surface Heat Flux

In this subsection, we address the question of the relation between mass flow and heat flux near the Earth's surface. In QG TEM formalism (Andrews *et al.* 1987),

$$\frac{\partial \bar{w}^p}{\partial t} - f_0 \bar{v}^r = \rho_0^{-1} \nabla \cdot \mathbf{F}_{EP} + \bar{F}_\lambda^p$$

where Cartesian geometry is assumed.  $f_0$  is the Coriolis parameter,  $\bar{v}^r$  is the residual meridional velocity,  $\mathbf{F}_{EP} \equiv (-\rho_0 \overline{v' u'^p}, \rho_0 f_0 \overline{v' \theta'^p} / \theta_{0z})$  is the Eliassen-Palm (EP) flux.  $\overline{(\cdot)^p}$  denotes zonal mean along isobars and here a prime ' is used again but to denote deviation from such an isobaric zonal mean.  $z$  is log-pressure height,  $\rho_0$  and  $\theta_{0z}$  are density and basic stratification in  $z$ -coordinates. The distribution of EP flux for the atmosphere shows that  $\mathbf{F}_{EP}$  practically points upward at the bottom of the atmosphere (Edmon *et al.* 1980). On the other hand, the streamlines of the residual circulation are clustered together in an infinitesimally thin surface boundary layer (Holton 1992), representing strong equatorward flow just above the surface. Hence, integrating vertically over the boundary layer of thickness  $\epsilon$ , only the dominant terms are left:

$$\int_0^\epsilon \rho_0 \bar{v}^r dz = -\frac{\rho_0}{\theta_{0z}} \overline{v' \theta'^p} \quad (30)$$

The above result shows, under QG scaling, poleward heat flux down the equator-pole temperature gradient on the surface forces a mean equatorward flow near the surface.

Held and Schneider (1999) have an similar explanation for the surface-zone equatorward flow in  $\theta$ -coordinates, paraphrased below: let  $\Delta m$  stand for the mass of a vertical column in the surface zone. Assume that geostrophic meridional wind  $v_g$  is uniform in the column, and isentropic density  $\sigma$  is constant in the surface zone. Thus,

$$\begin{aligned} v_g \Delta m &= v_g \sigma (\theta_{\max} - \theta_a) \\ \implies \overline{v_g \Delta m} &\approx -\sigma \overline{v_g' \theta_a'} \end{aligned} \quad (31)$$

where the horizontal average is taken along  $\theta = \theta_{\max}$  and so  $\overline{v_g} \equiv 0$  by definition.  $\theta_a'$  is the deviation in surface air potential temperature from its zonal mean. Comparing Eq. (30) and (31), Held and Schneider's explanation is basically the same as the explanation provided by QG TEM formalism if we assert QG balance and equate  $\sigma$  to  $\rho_0/\theta_{0z}$ .

Examining the premises of the above explanation in  $\theta$ -coordinates, vertical variations in  $v_g$  may perhaps be neglected in some parts of the surface zone due to vertical turbulent transport. But our model results show that the variations of  $\sigma$  in the surface zone, especially in the horizontal direction, is not negligible. So we need another explanation in  $\theta$ -coordinates that is valid generally for PE atmospheres.

The clue to relating surface heat flux to near-surface mass flow for PE atmospheres lies in the dynamical cause of the equatorward flow in the surface zone. In subsection (a), we explained that the flow is equatorward because of eastward surface form drag  $G_M$  which arises from equatorward migration of cold air and poleward migration of warm air at the bottom of the atmosphere. We shall next quantify this relation between surface form drag and surface heat flux.

Multiply Eq. (18) by  $\varpi$ , integrate with respect to  $\theta$  in the surface zone, convert to a zonal integral (cf. Fig. 6), integrate by parts, and note the relation in Appendix E,

$$\int_{\theta_{\min}}^{\theta_{\max}} \varpi G_M d\theta = \frac{-1}{2\pi} \int_0^{2\pi} \underset{\text{along the surface}}{M_a} \frac{\partial \theta_a}{\partial \lambda} d\lambda = \frac{1}{2\pi} \int_0^{2\pi} \underset{\text{along the surface}}{\theta_a} \frac{\partial M_a}{\partial \lambda} d\lambda = \frac{1}{2} f a \cos \varphi \overline{\nu v_g \theta_a^a} \quad (32)$$

$$\iota \equiv 1 + \frac{g}{f v_g} \frac{1}{a \cos \varphi} \frac{\partial z_s}{\partial \lambda} \quad (33)$$

where  $M_a \equiv M(\theta_a)$  is the surface value of  $M$ ,  $v_g \equiv (f a \cos \varphi)^{-1} (\partial M / \partial \lambda)_\theta$  is the geostrophic meridional wind,  $z_s$  is the surface terrain height, and  $\overline{(\cdot)^a}$  denotes zonal mean along the bottom surface of the atmosphere.  $\iota$  is a factor that depends on the steepness of the terrain:  $\iota \approx 1$  when the terrain gradient is much less than the ratio of Coriolis acceleration to gravitational acceleration ( $f v_g / g \sim 10^{-4}$  in mid-latitudes). As the model does not have any topography,  $\iota = 1$  and eastward surface form drag  $G_M$  in the surface zone in Fig. 4 is associated with poleward geostrophic potential temperature flux at the surface. Topography, even if present, enhances the eastward surface form drag, because anticyclones are generally associated with elevated terrain so that  $\iota > 1$  over mountain regions. Note that while QG scaling is not assumed, only the geostrophic wind is relevant to  $G_M$ . Thus, the explanation for eastward surface form drag is good even if the surface flow deviates significantly from geostrophy.

The factor of half on the RHS of equation (32) requires some explanation. The geostrophic potential temperature flux (suitably modified by topography if present) can be decomposed into mean and eddy components:  $\overline{\nu v_g^a \theta_a^a}$  and  $\overline{(\nu v_g)' \theta_a'^a}$ . These two

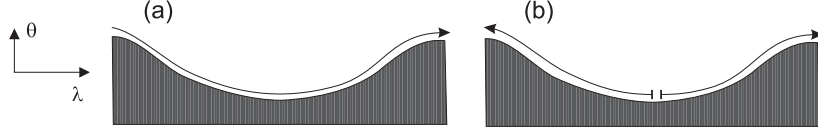


Figure 6. At the bottom surface of the atmosphere, (a) integration with respect to longitude  $\lambda$  is equivalent to (b) integration with respect to potential temperature  $\theta_a$ , with the integrand becoming a multi-valued function.

components are of comparable magnitudes as shown by the following scaling argument, where the atmosphere is disturbed from the basic thermodynamic state defined by  $\rho_0 \equiv \overline{\rho_a^a}$  and  $\theta_0 \equiv \overline{\theta_a^a}$ , and  $\rho_a$  and  $p_a$  are the density and pressure of surface air:

$$\begin{aligned} \nu v_g &= \frac{1}{\rho_a} \frac{\partial p_a}{\partial \lambda} \approx \frac{1}{\rho_0} \frac{\partial p_a'}{\partial \lambda} - \frac{\rho_a'}{\rho_0^2} \frac{\partial p_a'}{\partial \lambda} \\ \overline{\nu v_g^a \theta_a^a} &\approx -\frac{\rho_a'}{\rho_0^2} \frac{\partial p_a'^a}{\partial \lambda} \theta_0 \approx \frac{1}{\rho_0} \frac{\partial p_a'^a}{\partial \lambda} \theta_a' \approx \overline{(\nu v_g)'} \theta_a' \end{aligned}$$

Hence, one may think of the RHS of equation (32) as the average between mean and eddy transports of surface potential temperature. In the limit of small disturbances from a zonally uniform basic thermodynamic state, it just reduces to either the eddy or the mean transport. (cf. Schneider (2004) for an alternative formulation of equation (32) that does not have the factor of half above.)

Vertically integrate  $\varpi / \cos \varphi \times \text{Eq. (23)}$  (neglect relative torque) and use Eq. (32),

$$\int_{\theta_{\min}}^{\theta_{\max}} \overline{\sigma^S \overline{v}^*} \frac{f}{\overline{\sigma}} d\theta \approx -\frac{1}{2} f \overline{\nu v_g \theta_a^a} - \int_{\theta_{\min}}^{\theta_{\max}} \overline{\sigma v \uparrow \xi \uparrow^S} d\theta \quad (34)$$

Equation (34) is the generalization of Eq. (30) to PE atmospheres, allowing for vertical structure within a thick surface zone and taking into account the equatorward eddy PV flux responsible for the poleward flow that is sometimes present in the upper region of the surface zone. It is a rigorous statement that poleward heat flux at the surface drives equatorward mass-weighted mean flow in the surface zone at all times.

Since  $f/\overline{\sigma}$  is approximately the mass-weighted mean PV  $\overline{\xi}^*$ , Eq. (34) says that the total flux of PV effected by the mean flow and eddies in the surface zone must approximately cancel the the surface flux of potential temperature (which acts like a “surface potential vorticity”). Contrast this with the region above the surface zone where the total PV flux accelerates the mean flow on synoptic time-scales.

Our results highlight that the terrain-modified geostrophic potential temperature flux  $\overline{\nu v_g \theta_a^a}$  on the surface is to be parametrized in terms of the surface mean meridional potential temperature gradient, as part of Held’s explanation for the general circulation. The parametrization in Held (1999) involved the full eddy heat flux on a near-surface isobar.

### (c) General Circulation Dynamics

The time-average zonal average state of the model atmosphere over the period  $t = 105 \text{ d}$  to  $300 \text{ d}$  was analyzed in a similar fashion as in subsection (a). The results (not shown) are basically the same, apart from the fact that the relative torque is negligible because the model has equilibrated. Thus, above the surface zone, there is a balance

between eddy PV flux and Coriolis force, implying that  $\langle \bar{v}^* \rangle^*$  is determined effectively by eddy PV flux. Within the surface zone, mean pressure torque  $G_M$  forces a strong equatorward  $\langle \bar{v}^* \rangle^*$  in the lower region of the surface zone, while eddy PV flux forces a weaker poleward  $\langle \bar{v}^* \rangle^*$  in the upper region of the surface zone.

Let us try to understand the extratropical general circulation dynamics revealed above by the following simple scaling argument. Consider the identities

$$\langle \overline{v\zeta_\theta} \rangle \equiv \langle \bar{v} \rangle \langle \bar{\zeta}_\theta \rangle + \langle \overline{v'\zeta_\theta'} \rangle \quad (35)$$

$$\langle \overline{\sigma v\xi} \rangle \equiv \langle \bar{\sigma} \rangle \langle \bar{v}^* \rangle^* \langle \bar{\xi}^* \rangle^* + \langle \overline{\sigma v^\dagger \xi^\dagger} \rangle \quad (36)$$

(Recall that angular brackets denote time mean and the asterisk denote mass-weighting. Primes and daggers refer respectively to deviations from the unweighted and mass-weighted time mean zonal means in this context.)

In Eq. (35), as the contribution of planetary rotation to vertical absolute vorticity is dominant in the extratropics,  $\zeta_\theta \sim f$  and  $\langle \bar{\zeta}_\theta \rangle \sim f$ , and as  $\zeta_\theta'$  excludes the constant planetary contribution,  $\zeta_\theta' \ll f$ . Suppose  $v \sim V$ , the scale for meridional wind. Let  $v \equiv v_g + v_{ag}$  where  $v_g$  and  $v_{ag}$  are the geostrophic and ageostrophic velocities respectively. In the extratropics,  $v_{ag} \ll v_g$ . Above the surface zone,  $\bar{v}_g \equiv 0$  so that  $\langle \bar{v} \rangle \equiv \langle \bar{v}_{ag} \rangle \ll V$  and  $v' \sim V$ . Hence, by Eq. (35),  $\langle \overline{v\zeta_\theta} \rangle \ll fV$  above the surface zone.

In Eq. (36), the LHS is equivalent to the LHS of Eq. (35) and so is  $\ll fV$  above the surface zone. On the RHS,  $\langle \bar{\xi}^* \rangle^* \sim f \langle \bar{\sigma} \rangle^{-1}$  and we may now choose to define  $V \equiv \langle \bar{v}^* \rangle^*$ , so that the first term is  $\sim fV$ . Therefore, our scaling shows that above the surface zone, mean PV flux must approximately balance eddy PV flux, i.e.  $f \langle \bar{v}^* \rangle^* + \langle \overline{\sigma v^\dagger \xi^\dagger} \rangle \approx 0$ .

Within the surface zone,  $\langle \bar{v}_g \rangle$  varies from zero at the top to  $\sim V$  at the bottom. Thus,  $\langle \bar{v} \rangle \approx \langle \bar{v}_g \rangle \equiv -(fa \cos \varphi)^{-1} G_M$ . Apart from this fact, we may follow the same scaling as for above the surface zone and thus obtain

$$f \langle \bar{v}^* \rangle^* + \langle \overline{\sigma v^\dagger \xi^\dagger} \rangle \approx -(a \cos \varphi)^{-1} G_M \quad (37)$$

i.e. mean pressure torque  $G_M$  must balance total PV flux in the surface zone.

Integrating  $\langle \varpi \rangle^S \times$  Eq. (37) from the surface to the top of the atmosphere (noting that  $G_M = 0$  above the surface zone),

$$\int_{\theta_{\min}}^{\infty} \left( \langle \bar{\sigma} \rangle^S \langle \bar{v}^* \rangle^* \frac{f}{\langle \bar{\sigma} \rangle} + \langle \overline{\sigma v^\dagger \xi^\dagger} \rangle^S \right) d\theta + \frac{1}{2} f \langle \overline{\nu v_g \theta_a^a} \rangle^a \approx 0 \quad (38)$$

where  $\langle \cdot \rangle^a$  denote time mean at the Earth's surface. If we view  $f\theta_a$  as the areal concentration of "surface PV" (as opposed to "interior PV" concentration  $\sigma\xi$ ) and  $\nu v_g/2$  as the effective transport velocity of this surface PV, then Eq. (38) says that there is no net meridional PV transport in an atmospheric column. Above the surface zone, there is no net transport of PV meridionally along each isentrope. In the surface zone, interior PV is transported equatorward along isentropes to the surface by both mean flow and eddies but there is a compensating poleward transport of surface PV. (The interconversion between interior and surface PV is left as a topic for future research.) The explanation of the general circulation in terms of PV and surface heat transport is obtained because of the use of isentropic coordinates here.

Suppose the vertical integral in Eq. (38) reaches only a little above the tropopause, say  $\theta = \theta_{trp}^+$ , and  $\langle \bar{\sigma} \rangle$  is nearly vertically invariant in the troposphere. As mass density

above  $\theta_{trp}^+$  is small, we may take the tropospheric circulation as almost closed. Hence,

$$\int_{\theta_{\min}}^{\theta_{trp}^+} \langle \overline{\sigma v^\dagger \xi^\dagger}^S \rangle^S d\theta \approx -\frac{1}{2} f \langle \overline{v_g \theta_a}^a \rangle^a \quad (39)$$

Interior eddy PV flux in a tropospheric column (including that at the tropopause) is constrained by surface heat flux, and hence by surface potential temperature gradient.

It is instructive to compare the understanding of extratropical general circulation dynamics based on PV transport with an understanding based on angular momentum transport and form drag. Johnson (1989) showed that in the extratropics,

$$\frac{1}{\cos \varphi} \frac{\partial}{\partial \varphi} \langle \overline{\sigma^S v^* L^*} \cos \varphi \rangle^S \approx \langle \overline{\sigma^S} (F_D + F_S) a \cos \varphi \rangle^S \quad (40)$$

Thus, in the upper branch of the extratropical tropospheric meridional circulation, the angular momentum gained from the convergence of poleward mean angular momentum flux is conveyed via pressure stresses on isentropic surfaces into the lower branch of the circulation. The angular momentum thus gained by the lower branch of the circulation makes up for the loss due to divergence of the equatorward mean angular momentum flux there. Integrated over a vertical column of the atmosphere, the form drag term  $F_D$  vanishes, and so the net gain or loss in angular momentum of an atmospheric column depends mainly on the mountain drag  $F_S$  at the Earth's surface in the extratropics. This account is actually valid regardless of the vertical coordinate system used.

The explanations for extratropical general circulation dynamics in this paper and in Johnson (1989) represent two equivalent points of view. Johnson's view makes obvious the angular momentum exchange between the atmosphere and the lithosphere via mountain torques, and emphasizes the vertical redistribution of angular momentum by pressure stresses on isentropes. We offer an alternative PV- $\theta$  picture: mean and eddy PV transport along isentropes cancel above the surface zone; within the surface zone, the net (mean + eddy) isentropic flux of interior PV is cancelled by the surface flux of potential temperature. Thus, mean meridional flow (closely related to mean PV flux) is essentially driven by eddy PV flux and surface heat flux. Mass continuity implies that surface heat flux constrains tropospheric eddy PV flux.

#### (d) Structure of the Near-Surface Circulation

Fig. 7(a) shows the distribution of meridional mass flow  $\langle \overline{\sigma v^S} \rangle^S$  in the equilibrated model atmosphere. It shows an overturning circulation within the surface zone itself. The median potential temperature of surface air, referred henceforth as the "median line", divides the surface zone into an upper region and a lower region. The mass flow is largely antisymmetric about the median line. The antisymmetry is not perfect, because there is significant poleward flow at the tropopause level (not shown), implying a compensating net equatorward flow within the surface zone.

To explain the structure of the circulation within the surface zone, we use the isentropic zonal average formalism to adapt and modify the kinematic explanation of Held and Schneider (1999) (HS99 in this subsection). Mass flow in the surface zone is

$$\langle \overline{\sigma v^S} \rangle^S = \int_{\theta_{\min}}^{\theta} \mu(\theta_a) E \{ (\sigma v)_\theta \} d\theta_a \quad (41)$$

where  $\mu \equiv \partial \langle \varpi \rangle^S / \partial \theta$  and  $E \{ (\sigma v)_\theta \}$  is the expected value of the mass flow  $(\sigma v)_\theta$  at isentropic level  $\theta$  above the point where surface air has potential temperature  $\theta_a$  along

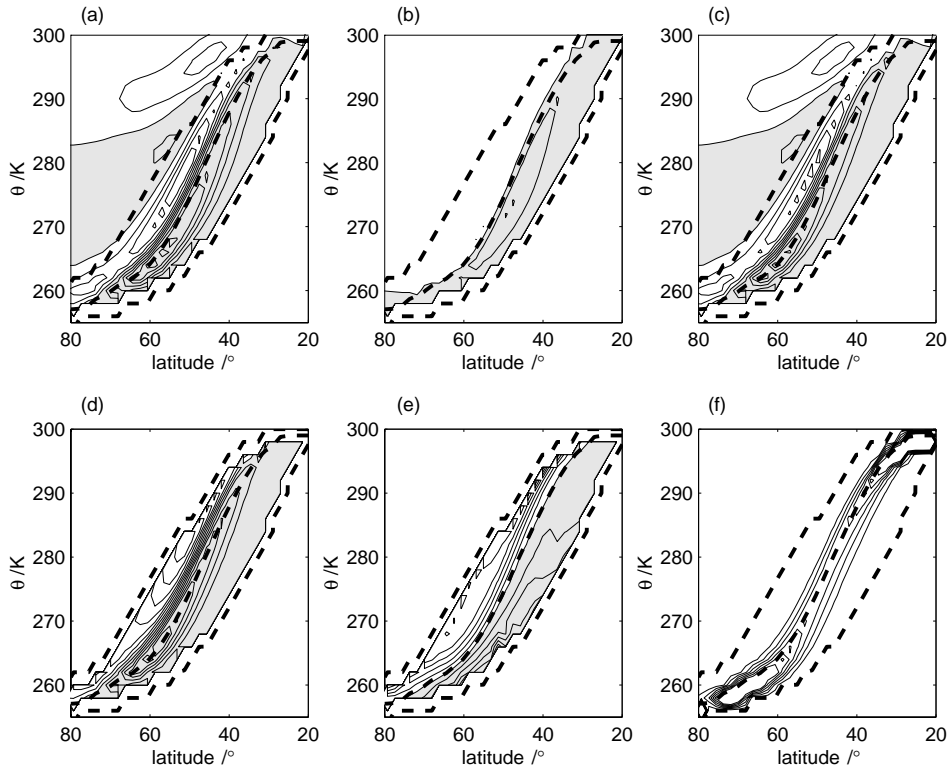


Figure 7. Meridional mass flow as a function of latitude and potential temperature (a) in the surface zone, and contributions from (b) the mixed layer and (c) above the mixed layer, i.e. respectively the three terms in Eq. (42). (d) is the meridional mass flow just above the mixed layer when surface air is potentially cooler than  $\theta$ , vis-a-vis the RHS of Eq. (43). Contours are at intervals of  $50 \text{ kg m}^{-1} \text{ K}^{-1} \text{ s}^{-1}$  in panels (a) to (d). (e) shows the expected value of meridional mass flow just above the mixed layer when surface air is at potential temperature  $\theta$ . The contour interval is  $500 \text{ kg m}^{-1} \text{ K}^{-1} \text{ s}^{-1}$ . (f) shows the probability density,  $\mu$ , of potential temperature of surface air, with contour interval  $0.03/\text{K}$  in the range  $0.03/\text{K}$  to  $0.18/\text{K}$ . In all panels, the surface zone is demarcated by the outer thick dashed lines, and the central thick dashed line in the surface zone is the ‘median line’ where  $\langle \varpi \rangle^S = 0.5$ . Shading denotes negative values.

latitude  $\varphi$ . The upper limit of the integral is  $\theta$  because when  $\theta_a > \theta$ , the isentropic level  $\theta$  does not exist in the atmosphere and so the expected mass flow at that level is zero.

If there is a mixed layer with uniform potential temperature  $(\theta_a + \epsilon)$  just above the bottom surface  $\theta_a$ , where  $\epsilon$  is positive and arbitrarily small, we may write the mass flow at isentropic level  $\theta$  as the sum  $V_{mix} \delta(\theta - \theta_a - \epsilon) + (\sigma v)_\theta \mathcal{H}(\theta - \theta_a - \epsilon)$ , where  $V_{mix}$  is the vertically integrated mass flow over the mixed layer,  $\delta$  is Dirac’s delta function and  $\mathcal{H}$  is the Heaviside step function. In the limit as  $\epsilon \rightarrow 0$ ,

$$\langle \overline{\sigma v}^S \rangle^S = \mu(\theta) E(V_{mix}) + \int_{\theta_{\min}}^{\theta} \mu(\theta_a) E\{(\sigma v)_\theta\} d\theta_a \quad (42)$$

where  $E(V_{mix})$  is the expected value of mass flux in the mixed layer wherever and whenever the mixed layer is at potential temperature  $\theta$ .

Fig. 7(b) and (c) show respectively the first and second terms on the RHS of Eq. (42). Mass flow through mixed layers are mainly equatorward and confined to the lower

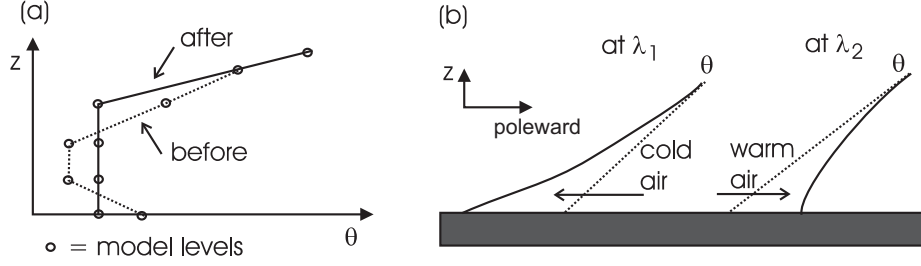


Figure 8. (a) Convective adjustment enhances static stability above the mixed layer. (b) Poleward advection of warm air enhances isentropic slope and vice versa for equatorward advection of cold air. Lines denote isentropes.

region of the surface zone, because mixed layers occur mostly when low- $\theta$  air moves equatorward over warm surface and becomes convectively unstable from surface heat transfer. The dominant contribution to  $\langle \overline{\sigma v}^S \rangle^S$  in the surface zone comes from above the mixed layer (cf. Fig. 7(a) and (c)).

As  $E\{(\sigma v)_\theta\}$  is a function of  $\varphi$ ,  $\theta$  and  $\theta_a$ , we shall make the approximation that the mass flow outside the mixed layer does not vary vertically in the surface zone so that  $(\sigma v)_\theta \approx (\sigma v)_{\theta_a^+}$ , where  $\theta_a^+$  is the potential temperature just above the mixed layer. This approximation is acceptable for our purpose, given the proximity of the distributions in Fig. 7(c) and (d). Thus,

$$\langle \overline{\sigma v}^S \rangle^S \approx \int_{\theta_{\min}}^{\theta} \mu(\theta_a) E\{(\sigma v)_{\theta_a^+}\} d\theta_a \quad (43)$$

where  $E\{(\sigma v)_{\theta_a^+}\}$  is a function of  $\varphi$  and  $\theta_a$  only (see Fig. 7(e)). Since the probability distribution  $\mu(\theta_a)$  is rather symmetric about the median line in the mid-latitudes (Fig. 7(f)), the antisymmetry in mass flow  $\langle \overline{\sigma v}^S \rangle^S$  about the median line must arise from symmetric contributions in  $E\{(\sigma v)_{\theta_a^+}\}$  according to Eq. (43). A priori, one might suppose  $E\{(\sigma v)_{\theta_a^+}\}$  to be antisymmetric about the median line based on the notion that cold air migrates equatorwards and warm air migrates polewards to accomplish equator-pole heat transfer. This notion is correct but it requires some refining as we show next.

Fig. 7(e) and (f) show that around the median line where  $\mu$  is significantly non-zero, the antisymmetry in  $E\{(\sigma v)_{\theta_a^+}\}$  is not perfect, i.e.

$$E\{(\sigma v)_{\theta_a^+}\} \approx \begin{cases} \alpha (\theta_a - \theta_m) & \text{if } \theta_a - \theta_m > 0 \\ \beta (\theta_a - \theta_m) & \text{otherwise} \end{cases} \quad (44)$$

where  $\theta_m$  is the median value of  $\theta_a$ , and  $\alpha \gg \beta > 0$ . Hence,  $E\{(\sigma v)_{\theta_a^+}\}$  manifests a strong symmetric component, explaining the strong antisymmetry in mass flow  $\langle \overline{\sigma v}^S \rangle^S$ . The dependence of  $E\{(\sigma v)_{\theta_a^+}\}$  on cold departures of  $\theta_a$  from  $\theta_m$  is weak because static stability (inversely related to  $\sigma$ ) is enhanced above mixed layers due to convection in cold-air outbreaks over warm surface (Fig. 8(a)). The different dependence of  $E\{(\sigma v)_{\theta_a^+}\}$  on warm and cold departures is also because isentropic slopes (directly related to  $\sigma$ ) are reduced in the equatorward advection of cold air and enhanced in the poleward advection of warm air at the surface (Fig. 8(b)).

The ideas embodied by Eq. (42) and (44) take after those expressed in HS99, except:

1. HS99 used the zonal mean rather than the median for  $\theta_m$ ;
2. they supposed that  $\sigma$  is constant in the surface zone outside the mixed layer;

3. they postulated that surface-zone meridional velocity is equally sensitive to warm and cold anomalies, i.e.  $\alpha = \beta$  in Eq. (44), given point 2;
4. they applied point 3 to mass flow in mixed layers as well, i.e.  $V_{mix} = \gamma (\theta_a - \theta_m)$  for all  $\theta_a$ , where  $\gamma$  is a positive constant.

Points 1 and 2 are minor differences that do not affect the essence of the argument here or in HS99; points 3 and 4 are pivotal points where we differ from HS99. Because of HS99's a priori assumption that  $\alpha = \beta$ , they deduce that surface-zone mass flow  $\langle \overline{\sigma v^S} \rangle^S$  must be symmetric about  $\theta_m$  in the absence of mixed layers. Thus, the antisymmetric component of  $\langle \overline{\sigma v^S} \rangle^S$  seen in their 50-year GCM integration was attributed to contributions from mass flow  $V_{mix}$  in mixed layers, which they assumed to be antisymmetric about  $\theta_m$ . Through the diagnostic formalism developed here, our model results show that HS99's points 3 and 4 are wrong: in fact,  $\alpha \gg \beta$  and  $V_{mix}$  is practically zero for  $\theta_a > \theta_m$ . Thus, mixed layers are not required to explain the strong antisymmetry in the surface-zone mass flow. Our results suggest that mixed-layer contributions are not important and may be ignored (i.e. Eq. (43)). Even when considered, mixed layers provide both symmetric and antisymmetric contributions.

Despite the above differences, the model results do show in accord with HS99 that the probability density  $\mu$  of surface air potential temperature is largely symmetric about some measure of average surface air potential temperature.

## 5. CONCLUSIONS

The isentropic zonal average formalism of e.g. Andrews (1983) is extended to include the lower boundary of the atmosphere as a "surface zone". In the surface zone, isentropes in the latitudinal plane are interrupted by the Earth's surface. The zonal average equations of motion in  $\theta$ -coordinates are Eq. (14), (19) and (20). Equation (8) describes the time-dependent lower boundary of the atmosphere, by relating the change in probability distribution  $\varpi$  of surface air potential temperature to expected values of diabatic heating and advection of potential temperature at the surface. Using a baroclinic wave model, we showed that the dominant forcing on the equatorward mean flow in the surface zone comes from surface form drag associated with the undulating bottom surface in  $\theta$ -coordinates (Eq. (18)). A time-average formulation of the isentropic zonal average formalism was also described to allow application in climatological diagnostics.

The relation between near-surface equatorward mean flow and surface poleward heat flux is evident in QG TEM formalism (Andrews and McIntyre 1976). We generalized this relation to PE atmospheres: equatorward surface-zone mean flow is forced by poleward surface potential temperature flux (Eq. (34)).

A PV- $\theta$  view of extratropical tropospheric circulation was presented. Haynes and McIntyre (1987) showed that there is no cross-isentropic PV transport. We showed that there is basically no zonal average isentropic PV transport above the surface zone, and likewise over the depth of the surface zone if we consider surface potential temperature as "surface PV". Eddy PV flux in a tropospheric column is constrained by surface  $\theta$  flux.

Held and Schneider (1999) attempted to explain the strong antisymmetric component in surface-zone mass flow about the zonal mean surface air potential temperature, by appealing to mass flow through mixed layers next to the surface. Their analytic argument is translated into the extended isentropic zonal average formalism (using the expectation operator E) and analyzed carefully with support from our model simulation. Our results show that mass flow through mixed layers is weak compared to mass flow above mixed layers, and so cannot be the main reason for the strong antisymmetry of the

mass flow in the surface zone. Instead, the main reason lies in the expected surface-zone mass flow being more sensitive to warm departures than to cold departures of surface air potential temperature from its median value.

While the significance of the near-surface equatorward flow has been highlighted before in the literature, the poleward flow in the surface zone has often been overlooked because it is contiguous with the poleward return flow above the surface zone. However, we wish to distinguish the poleward flow in the upper region of the surface zone from that above the surface zone. The reason is that flow in the surface zone is in contact with the Earth's surface. This means that the overturning circulation within the surface zone represents a quasi-horizontal circulation along the Earth's surface, where equatorward flow occurs in cold-air outbreaks at the surface and poleward flow occurs in warm sectors of surface cyclones, besides rising above cold air in frontal regions. The poleward flow within the surface zone is significant, because it provides a route for the recycling of air (and hence of trace gases and aerosols) next to the surface itself. It also highlights the significance of equatorward eddy PV flux just above the surface, in parallel with the familiar equatorward eddy PV flux at the tropopause level. Moreover, the poleward surface-zone flow has implications on the general circulation above the surface zone: the stronger it is, the weaker the complementing poleward quasi-isentropic flow must be above the surface zone in an equilibrated climate.

#### ACKNOWLEDGEMENTS

The authors would like to thank T. Schneider and I. M. Held for the discussions they have had. D. R. Johnson's comments on an earlier manuscript has been most helpful. This work was supported by National Science Foundation grant #ATM-98190992.

#### APPENDIX A

##### *Meaning of Term $G_A$*

Term  $G_A$  may be rewritten from Eq. (16) as

$$G_A = \frac{1}{2\pi\varpi} \sum_{j=1}^{2n} \int_{\lambda_j - \epsilon}^{\lambda_j + \epsilon} g_A[\lambda_j] u' a \cos \varphi d\lambda$$

$$g_A[\lambda_j] \equiv -\mathbf{u}_{edd} \cdot \nabla \mathcal{H} \left\{ (-1)^{j+1} (\lambda - \lambda_j) \right\}$$

where  $\mathcal{H}$  is the Heaviside step function and  $\mathbf{u}_{edd} \equiv (u', v', Q^\dagger)$  is the eddy velocity in  $\theta$ -coordinates. Since  $u' a \cos \varphi \nabla \mathcal{H} \{ (-1)^{j+1} (\lambda - \lambda_j) \}$  is the gradient of eddy angular momentum per unit mass at the Earth's surface (which is described locally by  $\lambda = \lambda_j(\varphi, \theta, t)$ ),  $G_A$  may be understood as the eddy advection of eddy angular momentum at the bottom boundary of the atmosphere.

#### APPENDIX B

##### *Meaning of Term $G_M$*

Insofar as horizontal acceleration in a hydrostatic atmosphere is concerned, Montgomery potential  $M$  in  $\theta$ -coordinates plays a similar role to pressure in geopotential height ( $z$ ) coordinates:  $-\nabla_\theta M \equiv -\rho^{-1} \nabla_z p$ . Thus, positive  $G_M \bar{\sigma}^S \delta\varphi \delta\theta$  is the eastward pressure torque that surface air  $\delta\varphi \delta\theta_a$  exerts on the isentropic tube  $\delta\varphi \delta\theta$ .  $G_M$  is like

the mountain torque exerted on the atmosphere by orography in  $z$ -coordinates, except that the ‘‘orography’’ in  $\theta$ -coordinates are variations in surface air potential temperature. Hence,  $G_M$  is an analogous ‘‘surface form drag’’ in  $\theta$ -coordinates.

$G_M$  is not actually equal to the physical form drag in geopotential height coordinates as  $-(\partial M/\partial \lambda)_\theta \sigma \delta \lambda \delta \varphi \delta \theta$  is only the part of zonal pressure torque exerted on the east-west faces of the isentropic fluid element  $\delta \lambda \delta \varphi \delta \theta$ . Zonal pressure torques exerted on other faces of the element are not present in  $G_M$ . In contrast,  $-(\partial p/\partial \lambda)_z \delta \lambda \delta \varphi \delta z$  is the entire zonal pressure torque exerted on the fluid element  $\delta \lambda \delta \varphi \delta z$ . Moreover,  $-(\partial M/\partial \lambda)_\theta$  is torque per unit mass but  $-(\partial p/\partial \lambda)_z$  is torque per unit volume.

## APPENDIX C

### *Details of the Numerical Model*

This appendix complements the description in Section 3. Order-6 zonal symmetry is imposed by retaining only zonal wavenumbers 0, 6, 12, 18, ... in the baroclinic-wave life-cycle experiments (Thorncroft *et al.* 1993). The full zonal spectrum is used in the long-time integration to obtain an equilibrated climate.  $\nabla^6$  hyperdiffusion with coefficient  $K_{hd} \equiv 2.91 \times 10^{26} \text{ m}^6 \text{ s}^{-1}$  is applied to relative vorticity, divergence and temperature to dissipate energy that cascades to high wavenumbers. Higher-resolution and lower-hyperdiffusion runs confirm the convergence of the presented numerical solutions.

Bulk aerodynamics formulae are employed to parametrize fluxes of horizontal momentum and potential temperature from the surface to the lowest model level, but the turbulent wind strength is set to a constant value,  $V_0 \equiv 10 \text{ m s}^{-1}$ . The drag coefficient  $C_d$  is chosen such that the damping time-scale on the PBL is  $\Delta / (C_d V_0) \equiv 1 \text{ d}$ , where  $\Delta$  is the thickness of the PBL (cf. Swanson and Pierrehumbert 1997). Vertical turbulent transport of momentum and potential temperature in the PBL are parametrized by an eddy-diffusion scheme, with the diffusivity increasing linearly from zero at the top of the PBL to the value  $K_e$  at the surface where the diffusion time  $\Delta^2 / K_e \equiv 1 \text{ d}$ . Surface temperature is a fixed function of latitude  $T_s(\varphi)$ , chosen to coincide with the initial basic state temperature in the lowest model level so that surface heat flux is zero initially.

The dry adiabatic adjustment scheme explained in Emanuel (1994) is adopted to represent the effects of convection. The scheme homogenizes potential temperature while conserving enthalpy in a convecting column.

Newtonian relaxation about a fixed equilibrium temperature  $T_{eq}(\varphi, \sigma)$  is used as a crude parameterization of radiative heating.  $T_{eq}$  is chosen to coincide with the initial basic state temperature so that radiative heating is zero at the starting time. A typical value  $\tau_{rad} \equiv 30 \text{ d}$  is chosen for the tropospheric radiative relaxation time.

## APPENDIX D

### *Mean Pressure Force and Form Drag on an Isentropic Layer*

In the algebra below, the first equality uses the chain rule; the second equality uses the  $M = \theta \Pi + \Phi$  and the chain rule; the third equality uses the expansion of the derivative of an integral with variable limits and the complete differential  $\delta \Gamma \equiv p \delta \Pi$ ; the last step uses  $\delta \Gamma = R \Pi \delta p / c_p$ , the ideal gas law, hydrostatic balance and the definition

$z_j \equiv z(t, \lambda_j, \varphi, \theta)$ .

$$\begin{aligned}
-\frac{\overline{\partial M^*}}{\partial \lambda} &= \frac{1}{g\bar{\sigma}^S} \overline{\left\{ \frac{\partial}{\partial \theta} \left( p \frac{\partial M}{\partial \lambda} \right) - p \frac{\partial \Pi}{\partial \lambda} \right\}}^S \\
&= \frac{1}{g\bar{\sigma}^S} \overline{\left\{ \frac{\partial}{\partial \theta} \left( p \frac{\partial \Phi}{\partial \lambda} \right) + \theta \frac{\partial}{\partial \theta} \left( p \frac{\partial \Pi}{\partial \lambda} \right) \right\}}^S \\
&= \frac{1}{\bar{\sigma}^S} \frac{\partial}{\partial \theta} \left( \overline{p \frac{\partial z^S}{\partial \lambda}} \right) + \frac{-1}{2\pi\bar{\sigma}^S} \sum_{i=1}^n \left[ p_j \frac{\partial z}{\partial \lambda} \frac{\partial \lambda_j}{\partial \theta} - \frac{\theta}{g} \frac{\partial \Gamma}{\partial \theta} \right]_{j=2i-1}^{j=2i} \\
\frac{-1}{a \cos \varphi} \frac{\overline{\partial M^*}}{\partial \lambda} &= \underbrace{\frac{1}{\bar{\sigma}^S} \frac{\partial}{\partial \theta} \left( \overline{\frac{p}{a \cos \varphi} \frac{\partial z^S}{\partial \lambda}} \right)}_{\equiv F_D} + \underbrace{\frac{-1}{2\pi\bar{\sigma}^S a \cos \varphi} \sum_{i=1}^n \left[ p_j \frac{\partial z_j}{\partial \theta} \right]_{j=2i-1}^{j=2i}}_{\equiv F_S}
\end{aligned}$$

Thus, the total form drag exerted on the isentropic layer  $\delta\theta$  by the surrounding atmosphere  $F_D \bar{\sigma}^S \delta\theta$  and by the Earth's surface  $F_S \bar{\sigma}^S \delta\theta$  is equal to the total pressure force  $-(a \cos \varphi)^{-1} \overline{(\sigma \partial M / \partial \lambda)}^S$ .

#### APPENDIX E

##### Relation used in Eq. (32)

Consider  $M_a \equiv M(t, \lambda, \varphi, \theta_a)$  so that

$$\overline{\theta_a \frac{\partial M_a}{\partial \lambda}}^a = \overline{\theta_a \left( \frac{\partial M}{\partial \lambda} \right)_\theta}^a + \overline{\theta_a \frac{\partial M}{\partial \theta} \frac{\partial \theta_a}{\partial \lambda}}^a$$

Since  $\partial M / \partial \theta = \Pi$ , the second term on the RHS above is equal to  $\overline{(M_a - g z_s) \partial \theta_a / \partial \lambda}^a$ , where  $z_s \equiv z(t, \lambda, \varphi, \theta_a)$ . Integrate this term by parts and rearrange the entire equation,

$$\overline{\theta_a \frac{\partial M_a}{\partial \lambda}}^a = \frac{1}{2} \overline{\theta_a \left\{ \left( \frac{\partial M}{\partial \lambda} \right)_\theta + g \frac{\partial z_s}{\partial \lambda} \right\}}^a$$

#### REFERENCES

- |   |      |   |
|---|------|---|
| Andrews, D. G.  | 1983 | A finite-amplitude Eliassen-Palm theorem in isentropic coordinates. <i>J. Atmos. Sci.</i> , <b>40</b> , 1877–1883   |
| Andrews, D. G., Holton, J. R. and Leovy, C. B.        | 1987 | <i>Middle Atmosphere Dynamics</i> . Academic Press, Inc., San Diego, USA  |
| Andrews, D. G. and McIntyre, M. E.                    | 1976 | Planetary waves in horizontal and vertical shear: The generalized Eliassen-Palm relation and the mean zonal acceleration. <i>J. Atmos. Sci.</i> , <b>33</b> , 2031–2048 |
| Bourke, W.  | 1974 | A multi-level spectral model I. Formulation and hemispheric integrations. <i>Mon. Weather Rev.</i> , <b>102</b> , 687–701   |
| Davis, C. A.  | 1997 | The modification of baroclinic waves by the rocky mountains. <i>J. Atmos. Sci.</i> , <b>54</b> , 848–868  |
| Dutton, J. A.   | 1976 | <i>The Ceaseless Wind</i> . McGraw-Hill, New York, USA  |
| Dunkerton, T. J.                                      | 1978 | On the mean meridional mass motions of the stratosphere and mesosphere. <i>J. Atmos. Sci.</i> , <b>35</b> , 2325–2333   |
| Edmon, H. J., Jr., Hoskins, B. J. and McIntyre, M. E. | 1980 | Eliassen-Palm cross sections for the troposphere. <i>J. Atmos. Sci.</i> , <b>37</b> , 2600–2616   |
| Emanuel, K. A.  | 1994 | <i>Atmospheric Convection</i> . Oxford university press, New York, USA  |
| Gallimore, R. G. and Johnson, D. R.                   | 1981 | A numerical diagnostic model of the zonally averaged circulation in isentropic coordinates. <i>J. Atmos. Sci.</i> , <b>38</b> , 1870–1890                               |

- Haynes, P. H. and McIntyre, M. E. 1987 On the evolution of vorticity and potential vorticity in the presence of diabatic heating and frictional or other forces. *J. Atmos. Sci.*, **44**, 828–841
- Haynes, P. H. and McIntyre, M. E. 1990 On the conservation and impermeability theorems for potential vorticity. *J. Atmos. Sci.*, **47**, 2021–2031
- Held, I. M. 1999 The macroturbulence of the troposphere. *Tellus*, **51A-B**, 59–70
- Held, I. M. and Hou, A. Y. 1980 Nonlinear axially symmetric circulations in a nearly inviscid atmosphere. *J. Atmos. Sci.*, **37**, 515–533
- Held, I. M. and Schneider, T. 1999 The surface branch of the zonally averaged mass transport circulation in the troposphere. *J. Atmos. Sci.*, **56**, 1688–1697
- Holton, J. R. 1992 *An Introduction to Dynamic Meteorology, 3rd ed.* Academic Press, Boston, Massachusetts, USA
- Hoskins, B. J. 1991 Towards a PV-theta view of the general circulation. *Tellus*, **43AB**, 27–35
- Hoskins, B. J., McIntyre, M. E. and Robertson, A. W. 1985 On the use and significance of isentropic potential-vorticity maps. *Q. J. R. Meteorol. Soc.*, **111**, 877–946
- Hoskins, B. J. and Simmons, A. J. 1975 A multi-layer spectral model and the semi-implicit method. *Q. J. R. Meteorol. Soc.*, **101**, 637–655
- Hoskins, B. J. and Valdes, P. J. 1990 On the existence of storm-tracks. *J. Atmos. Sci.*, **47**, 1854–1864
- Johnson, D. R. 1989 The forcing and maintenance of global monsoonal circulations: an isentropic analysis. *Advances in Geophysics*, **31**, 43–316
- Koh, T.-Y. 2001 ‘Isentropic diagnostics of mid-latitude circulation and transport’. PhD thesis, Massachusetts Institute of Technology
- Lee, S. and Held, I. M. 1993 Baroclinic wave packets in models and observations. *J. Atmos. Sci.*, **50**, 1413–1428
- Lorenz, E. N. 1955 Available potential energy and the maintenance of the general circulation. *Tellus*, **7** 157–167
- Magnusdottir, G. and Haynes, P. H. 1996 Wave activity diagnostics applied to baroclinic wave life cycles. *J. Atmos. Sci.*, **53**, 2317–2353
- Namias, J. 1940 *Air mass and isentropic analysis, 5th ed.* Am. Meteorol. Soc., Milton, Massachusetts, USA
- Schar, C. 1993 A generalization of bernoulli’s theorem. *J. Atmos. Sci.*, **50**, 1437–1443
- Simmons, A. J. and Hoskins, B. J. 1978 The life cycles of some nonlinear baroclinic waves. *J. Atmos. Sci.*, **35**, 414–423
- Schneider, T. 2004 Zonal momentum balance, potential vorticity dynamics, and mass fluxes on near-surface isentropes. *submitted to J. Atmos. Sci.*
- Shaw, W. N. 1930 *Manual of Meteorology. Vol III, The Physical Processes of Weather* Cambridge University Press, Cambridge, UK
- Starr, V. P. and White, R. M. 1951 A hemispherical study of the atmospheric angular-momentum balance. *Q. J. R. Meteorol. Soc.*, **77**, 215–225
- Swanson, K. L. and Pierrehumbert, R. T. 1997 Lower-tropospheric heat transport in the pacific storm track. *J. Atmos. Sci.*, **54**, 1533–1543
- Townsend, R. D. and Johnson, D. R. 1985 A diagnostic study of the isentropic zonally averaged mass circulation during the First GARP Global Experiment. *J. Atmos. Sci.*, **42**, 1565–1579
- Thorncroft, C. D., Hoskins, B. J. and McIntyre, M. E. 1993 Two paradigms of baroclinic-wave life-cycle behaviour. *Q. J. R. Meteorol. Soc.*, **119**, 17–55
- Tung, K. A. 1986 Nongeostrophic theory of zonally averaged circulation. Part I: Formulation. *J. Atmos. Sci.*, **43**, 2600–2618